Alzheimer's & Dementia: Translational Research & Clinical Interventions 5 (2019) 579-591

Featured Article

A single systemic inflammatory insult causes acute motor deficits and accelerates disease progression in a mouse model of human tauopathy

Megan Torvell[a,b,c,d], David W. Hampton[a,b], Peter Connick[e], Alasdair M. J. MacLullich[f], Colm Cunningham[g,*], Siddharthan Chandran[a,b,c,e,**]

[a]Centre for Clinical Brain Sciences, University of Edinburgh, Edinburgh, UK
[b]Euan MacDonald Centre for MND Research, University of Edinburgh, Edinburgh, UK
[c]UK Dementia Research Institute at University of Edinburgh, Edinburgh, UK
[d]UK Dementia Research Institute at University of Cardiff, Cardiff, UK
[e]The Anne Rowling Regenerative Neurology Clinic, University of Edinburgh, Edinburgh, Midlothian, UK
[f]Edinburgh Delirium Research Group, Geriatric Medicine, University of Edinburgh, Edinburgh, UK
[g]Trinity Biomedical Sciences Institute and Trinity College Institute of Neuroscience, School of Biochemistry and Immunology, Trinity College Dublin, Dublin, Ireland

Abstract

Introduction: Neuroinflammation, which contributes to neurodegeneration, is a consistent hallmark of dementia. Emerging evidence suggests that systemic inflammation also contributes to disease progression.

Methods: The ability of systemically administered lipopolysaccharide (LPS - 500 μg/kg) to effect acute and chronic behavioural changes in C57BL/6 and P301S tauopathy mice was assessed. Markers of pathology were assessed in the brain and spinal cord.

Results: P301S mice display regional microgliosis. Systemic LPS treatment induced exaggerated acute sickness behaviour and motor dysfunction in P301S mice compared with wild-type controls and advanced the onset and accelerated chronic decline. LPS treatment was associated with increased tau pathology 24 hours after LPS injection and spinal cord microgliosis at the end stage.

Discussion: This is the first demonstration that a single systemic inflammatory episode causes exaggerated acute functional impairments and accelerates the long-term trajectory of functional decline associated with neurodegeneration in a mouse model of human tauopathy. The findings have relevance to management of human dementias.

Keywords: Tau; Acute illness; Delirium; Systemic inflammation; Dementia; Alzheimer's disease; Microglia; LPS; IL-1

1. Introduction

Neuroinflammation is a consistent hallmark across neurodegenerative diseases and plays a pivotal role in the pathobiology of dementias. Genetic discoveries link Alzheimer's disease (AD) risk and inflammatory genes (CLU, CR1, PICALM, and TREM2) [1–7]. Peripheral inflammation also increases risk and rate of progression of dementia [8–10]. A prospective cohort study of mild-to-severe AD revealed that acute systemic inflammatory events doubled the rate of cognitive decline [11]. The mechanisms underlying systemic inflammation-mediated cognitive decline are unclear but interaction with primed microglia in the context of dementia may lead to acute deficits, including delirium, and long-term sequelae [12,13].

Others have shown that systemic inflammation exacerbates tau pathology. Repeated lipopolysaccharide (LPS)

The authors declare no conflicts of interest to disclose.

*Corresponding author. Tel.: 353-01-896-3964.
**Corresponding author. Tel.: 0131 242 9519.
E-mail addresses: colm.cunningham@tcd.ie (C.C.), siddharthan.chandran@ed.ac.uk (S.C.)

https://doi.org/10.1016/j.trci.2019.09.001

injection in 3xTg-AD mice did not affect amyloid pathology but dramatically increased microglial burden, IL-1β expression, and tau hyperphosphorylation [14]. The same regime exacerbated tau pathology in wild-type mice, while in hTau mice crossed to fractalkine (CX3CR1) knockouts (hTau-*CX3CR1*$^{-/-}$), LPS dose-dependently increased tau phosphorylation, suggesting it was microglia-mediated [15]. Intracerebral LPS in rTg4510 tau mice increased expression of microglial markers CD45, Arg-1, and YM1 and exacerbated tau pathology [16].

None of these studies tested impact of systemic inflammation on functional decline in the respective models. Accelerated decline was previously demonstrated in a prion disease model; wherein primed microglia produced exaggerated responses to LPS challenge, increasing microglial IL-1β, which contributes to sickness behaviour, acute working memory deficits, and accelerated progression of disease [12,17]. Recent studies in humans and mice support the hypothesis that the impact of systemic inflammation is influenced by the extent of underlying pathology [18].

In the present study, we investigate acute and chronic functional impacts of a single systemic inflammatory episode in the P301S tauopathy mouse model characterized by hyperphosphorylation and accumulation of misfolded tau, regional neuronal loss, astrogliosis, and microgliosis [19–21]. P301S tau mice or C57BL/6 controls were injected intraperitoneally with LPS and acute and chronic consequences were monitored. The findings demonstrate robust acute and chronic functional impacts of LPS, and increased AT8^{+}-tau pathology, which is independent of microglial priming but dependent on the underlying disease stage.

2. Methods

2.1. Animals

All procedures complied with UK Animals Scientific Procedures Act 1986 and local regulations. Animals were group-housed in environmentally enriched cages, with a 12-hour light/dark cycle, and access to food and water *ad libitum*. C57BL/6 animals were sacrificed at 8, 12, and 20 weeks and P301S at 8, 9, 10, 11, 12, 16, and 20 weeks, and in LPS studies either 24 hours after injection or at 22 weeks of age for immunohistochemistry.

2.2. LPS injections

Mice were injected intraperitoneally with 500 μg/kg lipopolysaccharide (LPS; *Salmonella enterica*, Sigma) or equivalent volume of saline. The chosen dose elicited a significant sickness and hypothermic response [22].

2.3. Behavioural tasks

Horizontal bar task: Mice were assessed weekly to establish baseline, and at 1 and 24 hours before and 6 and 24 hours after injection (10 or 16 weeks) and 36 hours after (16 weeks). Time taken for the mouse to either reach the platform or fall from the bar was converted to a score between 1 and 10 (Table 1). A maximum of 60 seconds was allowed to complete the task. Each mouse completed 3 trials per session and an average score was calculated.

Open field: Mice were tested 24 hours before and 4 hours and 24 hours after injection. Distance travelled was recorded for each mouse, expressed as percentage of distance travelled by saline controls and averaged for each group.

2.4. Immunostaining and histology

Animals were humanely euthanized with sodium pentobarbitone (Euthatal) and perfused with cold PBS and 4% paraformaldehyde. Brains and spinal cords (c5–c7) were removed, postfixed in 4% paraformaldehyde, cryoprotected in 25% sucrose, and then cryosectioned coronally at 25 μm and 16 μm, respectively. Cresyl-violet staining to identify neuronal cell bodies was performed after serial dehydration in alcohol. Antibodies used for immunostaining are listed in Table 2.

2.5. Immunofluorescence

Sections were rehydrated in 1% PBS, blocked, and permeabilized with 3% normal serum (NS, Vector Laboratories), 0.2% Triton-X100 (Tx; Sigma) where required, in PBS for 1 hour. Primary antibodies were applied in the same solution, overnight, slides washed, and incubated with biotinylated secondary antibodies in PBS/1%NS for 1.5 hours, followed by streptavidin-conjugated tertiary antibody in PBS containing bis-benzamide (1:4000, Sigma Aldrich) for 1.5 hours.

2.6. Diaminobenzidine staining

Nonspecific peroxidase activity was quenched with 1% H_2O_2 in methanol. For antigen retrieval, slides were incubated in citric acid (10mM, pH 6) for 10 minutes. Sections were washed, blocked with PBS/10%NS for 1 hour, and incubated with primary antibodies in PBS/10%NS overnight, then with biotinylated secondary antibody, ABC complex, and diaminobenzidine (DAB).

2.7. Quantitative analysis

Motor cortex superficial layers were imaged 0.75–1.25mm from midline of sections, 0.5–2.3mm rostral to bregma [23] using a Zeiss-A1 microscope with AxioVision 4.8 software. Cortical NeuN^{+}-, cresyl-violet^{+}-, GFAP^{+}-, and IBA1^{+}-cells were counted in at least 4 sections/animal. A standard grid was drawn, cells counted up to 150μm depth and expressed as cells/mm^2. DAB-stained GFAP^{+}-cell counts were conducted in spinal cord lamina 9 in a 400μm × 200 μm grid. Stitched brightfield images of the whole IBA1 DAB-stained spinal cord were generated using

Table 1
Horizontal bar score

Score	Time to fall (s)	Score	Time to platform (s)
0	0–5	10	0–5
1	6–10	9	6–10
2	11–20	8	11–20
3	21–40	7	21–30
4	41–59	6	31–59
5	60	5	60

the Panavision tool in AxioVision. IBA1$^+$-cell counts were conducted in a 200 μm × 200 μm grid positioned over ventral horn lamina 9.

2.8. Automated analyses

ImageJ/Fiji software [24,25] was used for automated image analysis. A macro was used to batch process images; steps were as follows: (1) subtract background; (2) impose intensity threshold; (3) create binary mask; (4) select area of interest; (5) count objects. Parameters were determined by iterative optimization on randomly selected images before batch processing.

2.9. ELISA and qPCR

C57BL/6 and P301S mice were euthanized at 16 weeks of age, 4 hours after injection with LPS or saline. Serum and tissue were harvested. IL-1β and TNF-α serum levels were quantified by ELISA (DuoSet; R&D Systems) according to manufacturer's protocols. For RNA isolation, 20–40 mg cortex and spinal cord samples (c5–c7) were lysed and homogenized in QIAzol Lysis Reagent (79306, Qiagen). Total RNA was extracted using Qiagen RNeasy Mini Kit; TURBO DNA-free™ Kit (Ambion Life Technologies) was used to remove DNA contamination. Thermo Scientific DyNAmo cDNA Synthesis Kit was used for reverse transcription. Thermo Scientific DyNAmo Flash SYBR Green qPCR Kit was used in a 96-well format with 15 μl reaction volume for quantitative (Q)-PCR (10 minutes at 95°C followed by 40 cycles of 10 seconds at 95°C, 40 seconds at 60°C, 30 seconds at 72°C). Primers were designed (across introns where possible) using Primer Express software (Applied Biosystems). Primer and probe sequences are shown in Table 3. Assays were quantified using a relative standard curve and normalized to ribosomal RNA 18S expression. Relative abundance of mRNA in groups was calculated by the comparative C_T method [26].

2.10. Statistics

Mixed-effects linear regression (LR) with random intercept for animal ID was used for within-time-point comparison of P301S with C57BL/6 mice (immunostaining, histology, and qPCR). To investigate the trajectory of increasing pathology and decline in horizontal bar performance, an additional dummy variable was created for "age in weeks" to recenter data. For LPS studies, an additional term for LPS treatment was used for comparison of C57BL/6 and P301S mice treated with either saline or LPS. Custom hypothesis tests were used to generate estimated means and SEMs for graphs. An interaction term was generated to determine whether LPS had a greater effect on P301S mice than controls. This analysis was used for ELISA, qPCR, immunostaining, and within-time-point open-field and acute horizontal bar data. Piecewise LR was used with random intercept for ID to compare the longitudinal trajectory of horizontal bar performance of the groups.

3. Results

3.1. Progressive neuronal loss in superficial motor cortex and spinal cord of P301S mice

We sought to define the temporal pathological and behavioural trajectory of disease progression to determine optimal points to induce systemic inflammation. Noting earlier findings of cortical neuronal loss [19], we undertook cresyl-violet$^+$-counts in motor cortex superficial layers at 8, 9, 10, 11, 12, 16, and 20 weeks of age (Fig. 1A–E). Neuronal density of control mice was unchanged across all ages. Cresyl$^+$-cell

Table 2
Antibodies used

Antibody	Cat #	Dilution	Origin
Moue monoclonal anti-NeuN	MAB377B	1:400	Merck Millipore
Rabbit polyclonal anti-GFAP (glial fibrillary acidic protein)	Z0334	1:1000	DAKO
Rabbit polyclonal anti-IBA1	MP-290-CR05	1:1000	A. Menarini Diagnostics
Goat polyclonal anti-IBA1	Ab5076	1:1000	AbCam
Mouse monoclonal anti-phospho-tau (AT8)		1:1000	Autogen Bioclear
Goat anti-rabbit IgG (H+L) biotinylated	B2770	1:1000	Thermo Fisher Scientific
Donkey anti-goat IgG (H+L) biotinylated	A16003	1:1000	Thermo Fisher Scientific
Horse anti-mouse/rabbit IgG (H+L) biotinylated	BA-1400	1:200	Vector Laboratories
Streptavidin conjugated Alexa 488	S32354	1:1000	Thermo Fisher Scientific
Streptavidin conjugated Alexa 568	S11226	1:1000	Thermo Fisher Scientific
Goat anti-rabbit IgG (H+L) Alexa Fluor 488	A11008	1:1000	Thermo Fisher Scientific
Goat anti-mouse IgG (H+L) Alexa Fluor 568	A11004	1:1000	Thermo Fisher Scientific

Table 3
Primers supplied by Sigma (Poole, UK)

Target	Accession no.	Forward	Reverse
18S	NR_003278.3	5′- CCCAGTAAGTGCGGGTCAT-3′	5′- CCGAGGGCCTCACTAAACC-3′
Axl	NM_001190974.1	5′-TGAAGCCACCTTGAACAGTC-3′	5′-GCCAAATTCTCCTTCTCCCA-3′
Clec7a	NM_020008.3	5′-CCCAACTCGTTTCAAGTCAG-3′	5′-AGACCTCTGATCCATGAATCC-3′
Il1b	NM_008361.4	5′- TGCCACCTTTTGACAGTGATG-3′	5′- TGATGTGCTGCTGCGAGATT-3′
Itgax	NM_021334	5′-CTGGATAGCCTTTCTTCTGCTG-3′	5′-GCACACTGTGTCCGAACTC-3′
Tyrobp	NM_011662.2	5′-CGTACAGGCCCAGAGTGAC-3′	5′-CACCAAGTCACCCAGAACAA-3′

density in P301S mice was significantly reduced compared with controls from 11 weeks onward (Fig. 1E). As the dominant motor phenotype of P301S mice is progressive hind-limb paralysis due to ventral spinal cord motor neuron loss, we next quantified neuronal loss in spinal cord lamina 9; significant loss of $NeuN^+$-cells was apparent at 20 weeks (Fig. 1F–J).

GFAP quantification for astrogliosis in the cortex or spinal cord showed stable expression in C57BL/6 mice across all ages studied. There was significant cortical astrogliosis in P301S mice even at 8 weeks of age compared with controls. Mixed-effects LR from 8 to 20 weeks of age revealed progressive cortical astrogliosis, with average increase of 10.4 $GFAP^+$-cells/mm^2/week ($P < .001$; 95% CI 6.2 to 14.6; Fig. 1K–O). Astrogliosis in the ventral horn of the spinal cord was elevated in P301S mice compared with controls at 8 weeks and showed progression at 19.9 cells/mm^2/week ($P < .001$; 95% CI 14.2 to 25.; 6Fig. 1P–T).

3.2. P301S mice display regional heterogeneity of microgliosis

Despite accumulation of hyperphosphorylated tau, neuronal loss, and astrogliosis in the motor cortex, quantification of $IBA1^+$-cells showed no difference in microglial numbers in motor cortices of controls versus P301S mice at any time point (Fig. 2A–E); however, there was progressive microgliosis, associated with altered morphology, in spinal cord lamina 9 of P301S mice, significant compared with controls from 10 weeks of age (Fig. 2F–J). Microglial activation status was examined by qPCR for markers of priming and density (Fig. 2K). Motor cortex *Itgax* (cd11c) mRNA levels were elevated (1.8-fold) in P301S mice relative to controls at 16 weeks but there were no significant differences in *Axl*, *Tyrobp*, *or Clec7a.* By contrast, all microglial activation markers were significantly elevated in P301S spinal cords compared with controls: *Axl* (1.4-fold); *Tyrobp* (1.9-fold); *Itgax* (14.9-fold); *Clec7a* (5.8-fold), demonstrating regional heterogeneity of microgliosis in P301S mice (Fig. 2K).

3.3. Defining disease progression using horizontal bar performance

Noting that P301S mice develop progressive hind-limb paralysis [20], we identified the horizontal bar task as optimal to evaluate disease progression. Motor function of control mice remained constant throughout the experiment, whereas P301S mice exhibited a stable phase between 10 and 15 weeks and a declining phase between 15 and 21 weeks (−0.9 Δ points/week; $P < .001$; 95% CI −1.1 to −0.8; Fig. 3A).

3.4. LPS injection caused exaggerated acute behavioural and pathological responses in P301S mice

To assess the influence of underlying disease stage on the impact of acute systemic inflammation, LPS was given i.p., either early (10 weeks), immediately preceding demonstrable neuronal loss in P301S mice, or late (16 weeks), at the point of inflection in the functional decline curve (Fig. 3A), when neuronal loss, astrogliosis, and microgliosis were already established. Both C57BL/6 and P301S mice showed reduced locomotor activity in open field at 4 hours after LPS injection, but while C57BL/6 mice completely recovered by 24 hours, P301S mice showed persistently reduced locomotor activity (∼50% when injected at 10 or 16 weeks vs. ∼95% in C57BL/6; Fig. 3B). Because effects of treatments at 10 and 16 weeks were statistically indistinguishable on all behavioural tasks, at every time point assessed for C57BL/6+saline, C57BL/6+LPS, and P301S+saline, these 10- and 16-week groups were pooled in these 3 cases (for nonpooled data, see Supplementary data).

3.5. LPS injection causes an exaggerated deficit in horizontal bar performance of P301S mice

P301S mice showed exaggerated acute deficits in horizontal bar performance in the hours after LPS injection in an age-dependent manner (Fig. 3C). Before injection at either 10 or 16 weeks of age, there was no difference in performance between groups. Saline injection had no effect on acute performance in P301S or C57BL/6 mice regardless of age at injection (Fig. 3C); LPS injection had marginal influence on performance in C57BL/6 mice 6 hours after injection (Fig. 3C) but robustly impaired task performance of P301S mice when injected at 10 or 16 weeks (Fig. 3C). P301S mice injected at 16 weeks took longer to recover than those injected at 10 weeks, suggesting that progressive tau pathology increased vulnerability to these acute deficits (Fig. 3C). Except for those from P301S+LPS, data from 10

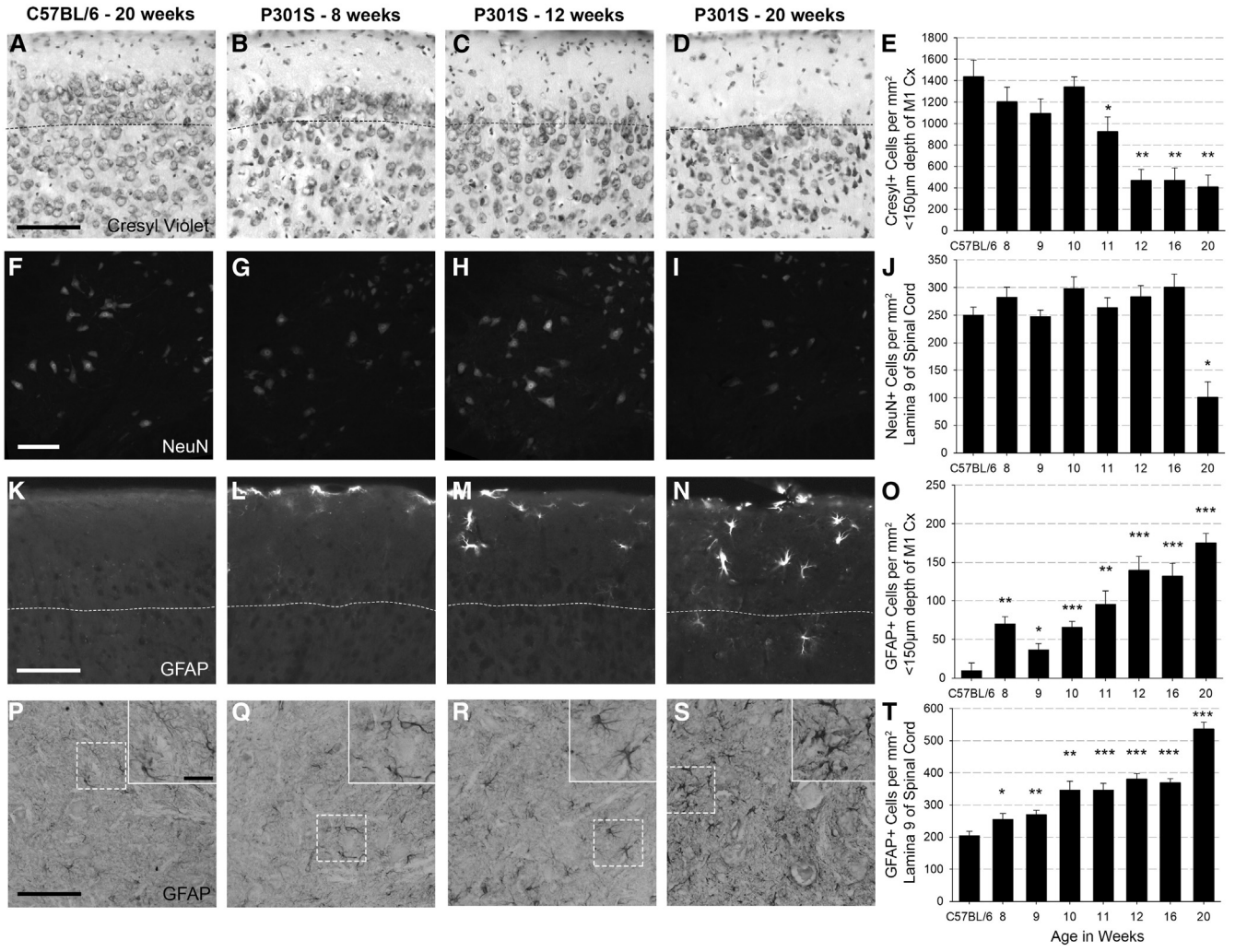

Fig. 1. Cell counts show progressive reduction in neuronal density in the superficial cortex and spinal cord accompanied by progressive astrogliosis: Representative examples of cresyl-stained cortical tissue (A–D), NeuN-stained spinal cord (lamina 9 of c5–c7) (F–I), GFAP-stained cortical tissue (K–N), and GFAP-stained spinal cord (lamina 9 of c5–c7), with in-lay to show morphology (P–S) from a 20-week-old C57BL/6 mouse and P301S mice at 8, 12, and 20 weeks. (E) Cresyl^{+}-cell counts in the cortex (to subpial depth of 150 µm) indicate neuronal loss from 11 weeks onward (-514.2 Δcells/mm^2; $P = .036$; 95% CI -982.0 to -46.3). C57BL/6 n = 4, P301S 8 wk n = 5, 9 wk n = 7, 10 wk n = 7, 11 wk n = 4, 12 wk n = 5, 16 wk n = 5, 20 wk n = 5. (J) NeuN^{+}-cell counts demonstrate neuronal loss in lamina 9 at 20 weeks (-148.3 Δ cells/mm^2; $P < .001$; 95% CI -214.1 to -82.5). C57BL/6 n = 13, P301S numbers as above. (O) GFAP^{+} cell counts in the motor cortex (to subpial depth of 150 µm) showed astrogliosis in P301S mice from 8 weeks onward. C57BL/6 n = 8, P301S 8 wk n = 5, 9 wk n = 5, 10 wk n = 5, 11 wk n = 5, 12 wk n = 5, 16 wk n = 5, 20 wk n = 4. (T) GFAP^{+} cell counts in lamina 9 of the spinal cord showed astrogliosis at 8 weeks (mixed-effects LR indicated by $*P < .05$, $**P < .005$, $***P < .0001$). Evaluation of time course confirmed that astrogliosis in the cortex and spinal cord was progressive. C57BL/6 n = 8, P301S 8 wk n = 4, 9 wk n = 4, 10 wk n = 3, 11 wk n = 4, 12 wk n = 5, 16 wk n = 5 20 wk n = 4. Dotted lines mark 150 µm subpial depth. Scale bars represent 100 µm, in-lay scale bar represents 25 µm. Analyses were by mixed-effects LR; $*P < .05$, $**P < .005$, $***P < .0001$. Abbreviation: LR, linear regression.

and 16 weeks were pooled, as described previously, for clarity of presentation. The statistical significance of effects of LPS on horizontal bar performance in P301S mice was not dependent on pooling of data (for nonpooled data, see Supplementary data).

3.6. LPS injection caused comparable levels of peripheral inflammation in P301S and control mice

To assess inflammatory status during LPS challenge and whether challenge triggered de novo pathology, a cohort of C57BL/6 and P301S mice were sacrificed 4 or 24 hours after injection. Serum collected 4 hours after injection was assayed for TNF-α and IL-1β. TNF-α was below assay detection in all saline-injected animals (Fig. 3D) and IL-1β levels were reduced in P301S relative to C57BL/6 mice ($P < .001$-Fig. 3E) indicating that P301S tauopathy per se does not induce systemic cytokines. TNF-α and IL-1β levels were increased to similar degrees after LPS injection in C57BL/6 and P301S mice ($P < .001$ for each analyte-Fig. 3D,E).

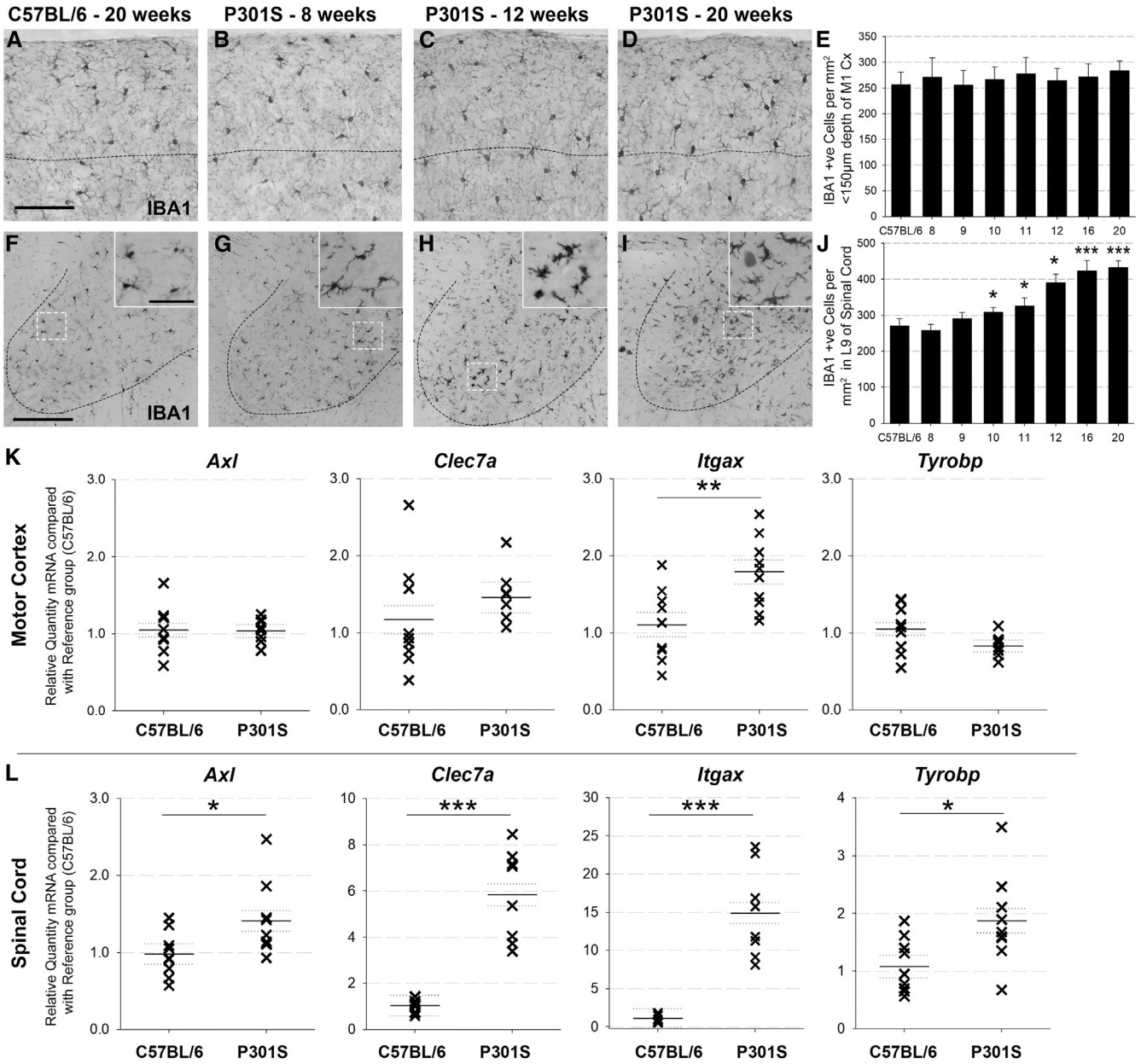

Fig. 2. P301S mice display regional heterogeneity of microgliosis: Representative examples of IBA1-stained cortical tissue (A–D) and spinal cord (lamina 9) (F–I) from a C57BL/6 mouse at 20 weeks, and P301S mice at 8, 12, and 20 weeks. Dotted line marks 150 µm subpial depth, and scale bar represents 100 µm (A–D). Dotted line marks ventral horn, scale bar represents 200 µm, and in-lay scale bar represents 25 µm (F–I). (E) IBA1$^+$ cell counts conducted in the motor cortex (to subpial depth of 150 µm) showed no difference between C57BL/6 and P301S mice at any age and no change over time. C57BL/6 n = 13, P301S 8 wk n = 4, 9 wk n = 3, 10 wk n = 6, 11 wk n = 5, 12 wk n = 5, 16 wk n = 6 20 wk n = 5. (J) IBA1$^+$ cell counts in lamina 9 of the spinal cord indicated regional microgliosis in P301S mice from 10 weeks onward. Time-course analysis showed that microgliosis was progressive (increase of 15.5 IBA1$^+$ cells/mm^2/week, $P < .001$; 95% CI 11.1 to 19.8). C57BL/6 n = 15, P301S 8 wk n = 6, 9 wk n = 3, 10 wk n = 7, 11 wk n = 4, 12 wk n = 3, 16 wk n = 5; 20 wk n = 4. (K) The relative quantity of *Itgax* mRNA ($P = .007$; 95% CI 0.2 to 1.2) but not *Axl, Clec7a*, and *Tyrobp* mRNA was elevated in P301S vs. C57BL/6 cortex. (L) All 4 genes were elevated in the spinal cords of P301S compared with C57BL/6 mice: *Axl* (1.4-fold, $P = .035$; 95% CI 0.0 to 0.8), *Itgax* (14.9-fold, $P < .001$; 95% CI 9.9 to 17.8), *Clec7a* (5.8-fold, $P < .001$; 95% CI 3.4 to 6.2), and *Tyrobp* (1.9-fold, $P = .014$; 95% CI 0.2 to 1.4) (all groups n ≥ 8). Analyses were by mixed-effects LR; *$P < .05$, **$P < .01$, ***$P < .001$. Abbreviation: LR, linear regression.

Il1b mRNA transcription in the motor cortex and spinal cord of P301S mice was not different from C57BL/6 controls (Fig. 3F); however, LPS injection increased *Il1b* 22.4-fold in C57BL/6 mice ($P < .001$) compared with 9.5-fold in P301S mice ($P < .001$). The interaction term indicated that LPS had a significantly smaller impact on P301S mice than C57BL/6 mice (relative quantity −11.9; $P = .002$; 95% CI −18.7 to −5.0). The same trend was found in the spinal cord: *Il1b* was equivalent in P301S mice and C57BL/6 mice (Fig. 3G), while LPS injection increased *Il1b,* in both groups and to a smaller degree in P301S mice (relative quantity −52.1; $P = .023$; 95% CI −96.1 to −8.14). These data

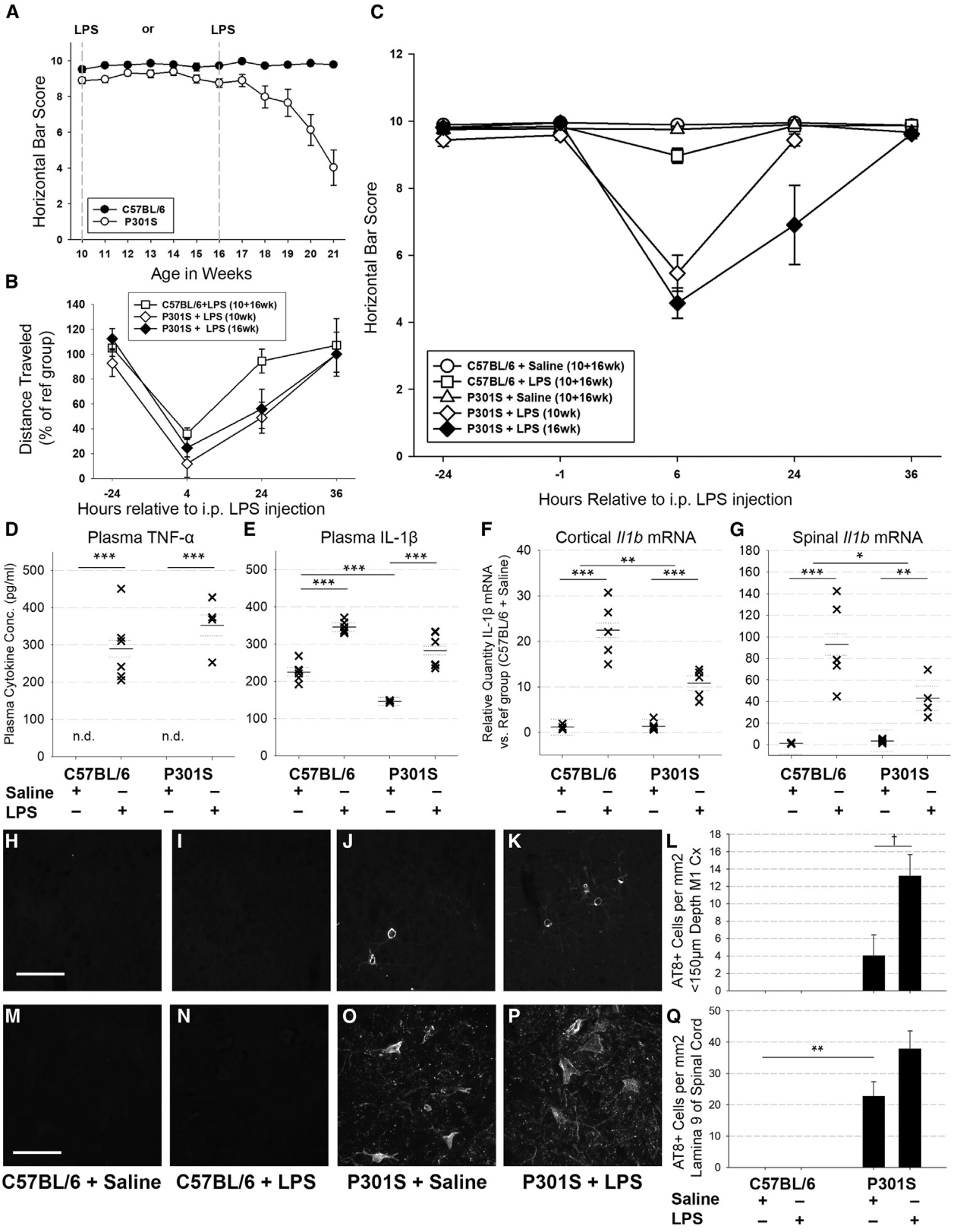

Fig. 3. LPS injection caused an exaggerated acute behavioural and pathological response in P301S mice: (A) Horizontal bar performance of C57BL/6 (-●-) is stable throughout 10–21 weeks (0.0 Δ points/week; $P = .728$; 95% CI −0.1 to 0.1). P301S mice (-○-) displayed a stable phase (10–16 weeks), followed by a declining phase (16–21 weeks) during which they lost 0.9 points/week ($P < .001$; 95% CI −1.1 to −0.8) (up to 20 weeks: n = 15/group; 21 weeks: n = 12/group). C57BL/6 and P301S mice were injected with LPS (i.p., 500 µg/kg) or saline at 10 or 16 weeks of age (indicated by grey lines). (B) Distance travelled in the open-field chamber by LPS-injected mice is expressed as a percentage of distance travelled by saline-injected counterparts. Four hours after injection, LPS

suggest that microglia are not primed by tau exposure and may even be desensitized.

3.7. LPS injection increases tau pathology in P301S mice

To test whether LPS injection at 16 weeks acutely increased tau pathology, AT8$^+$-neurons were counted. C57BL/6 controls had no AT8$^+$-neurons in the motor cortex regardless of LPS exposure (Fig. 3H–L); however, AT8$^+$-cells were detected in the motor cortex and spinal cord of P301S mice and were increased 24 hours after LPS treatment in the motor cortex (Fig. 3H–L) and spinal cord (Fig. 3 M-Q).

3.8. Systemic inflammation exacerbates the trajectory of functional decline

After a single LPS injection, all groups of mice showed impaired horizontal bar performance that recovered after resolution of the acute sickness response (Fig. 3C). Thereafter, C57BL/6 mice maintained baseline performance throughout the rest of the experiment, regardless of whether they were injected early or late with saline or LPS (Fig. 4). LPS injection at 10-weeks did not statistically influence long-term decline in P301S mice. By contrast, task performance of P301S mice injected with LPS at 16 weeks fell by ∼0.9 points/week between 16 and 22 weeks of age ($P < .001$–Fig. 4). For clarity of presentation, data from 10 and 16 weeks were pooled in all groups except P301S+LPS, as described previously. The statistical significance of the accelerated decline was not dependent on pooling of data (for nonpooled data, see Supplementary data). Therefore, the underlying disease stage significantly influences the impact of an acute systemic inflammatory insult.

3.9. Neuropathological changes correlate with exacerbated decline

Saline-injected P301S mice showed significantly greater neuronal loss (NeuN) in the superficial layers of the cortex and spinal cord compared with C57BL/6 mice (Fig. 5A–D) at 22 weeks of age. LPS injection caused equivalent loss of NeuN$^+$-cells in the cortices of C57BL/6 mice and P301S mice (Fig. 5A, B), but no losses were observed in the spinal cord (Fig. 5C, D). IBA1$^+$-microglial counts in the superficial layers of the cortex were not significantly different between any of the groups (Fig. 5E, F). Conversely, there was significant microgliosis in the spinal cord lamina 9 in P301S mice compared with controls ($P < .001$–Fig. 5G, H), and LPS injection at 16 weeks significantly increased microgliosis in P301S (but not control) spinal cords at 22 weeks ($P = .003$) (Fig. 5G, H).

No AT8$^+$-neurons were observed in the motor cortex or spinal cord of C57BL/6 mice regardless of LPS exposure (Fig. 5I, J); P301S mice had abundant AT8$^+$-cells in both regions at 22 weeks ($P < .001$), but LPS treatment at 16 weeks had no significant impact on AT8$^+$ numbers in either region.

4. Discussion

We have shown that a single systemic inflammatory event causes exaggerated acute functional deficits and accelerated disease-associated functional decline in the P301S mouse model of tauopathy, particularly when applied later in disease. This demonstrates that mice with aggregated tau pathology become progressively more vulnerable to deleterious consequences of acute inflammatory insults. There was stark regional heterogeneity of microgliosis, progressive and robust in the spinal cord but absent in the cortex despite presence of cortical tau aggregates and neuronal loss.

impacted open-field activity of C57BL/6 and P301S mice. Twenty-four hours after injection, LPS-injected C57BL/6 mice had recovered (-□-), while P301S injected with LPS at 10 or 16 weeks had not: P301S+LPS (10 wk: -◇-) travelled 51.1% less than saline-injected counterparts ($P = .002$; 95% CI −83.2 to 18.9) and P301S+LPS (16 wk: -◆-) travelled 43.9% less than saline-injected counterparts ($P = .015$; 95% CI −78.9 to 9.0). (C57BL/6+saline n = 18, C57BL/6+LPS n = 18, P301S+saline n = 16, P301S+LPS (10 wk) n = 9, P301S+LPS (16 wk) n = 7). (C) LPS significantly impacted horizontal bar performance 6 hours after injection in C57BL/6 and, to a greater degree, P301S mice; the magnitude of the effect was not impacted by age at injection (C57BL/6+LPS (-□-): −0.9 Δ points; $P = .02$; 95% CI −1.5 to −0.4; P301S+LPS (10 wk) (-◇-): −4.3 Δ points; $P < .001$; 95% CI −5.0 to −3.6, P301S+LPS (16 wk) (-◆-): (−5.2 Δ points; $P < .001$; 95% CI −6.0 to −4.4). At 24 hours after LPS injection, there was a differential impact of age of injection for P301S mice (C57BL/6+LPS (-□-): P = n.s; P301S+LPS (10 weeks) (-◇-): −0.5 Δ points; $P = .155$; 95% CI −1.1 to 0.2; P301S+LPS (16 weeks) (-◆-): −3.0 Δ points; $P < .001$; 95% CI −3.8 to −2.2). (C57BL/6+saline n = 19, C57BL/6+LPS n = 22, P301S+saline n = 21, P301S+LPS (10 wk) n = 13, P301S+LPS (16 wk) n = 7). Plasma TNF-α (D) and IL-1β (E) concentrations from C57BL/6 or P301S mice injected with saline or LPS, at 16 weeks, were measured 4 hours after injection. TNF-α levels were below detection in saline-injected animals but LPS injection increased TNF-α plasma levels in both groups (C57BL/6+LPS: +290.3 Δpg/ml; *$P < .001$; 95% CI 222.3 to 358.3; P301S+LPS: +352.3 Δ pg/ml; *$P < .001$; 95% CI 288.9 to 415.7). (C57BL/6+saline n = 6, C57BL/6+LPS n = 6, P301S+saline n = 6, P301S+LPS n = 4). (E) Plasma IL-1β was reduced in P301S mice versus C57BL/6 mice (-79.3 Δpg/ml; *$P < .001$; 95% CI -112.8 to -45.8). LPS injection increased IL-1β levels for both genotypes (C57BL/6+LPS: +120.4 Δpg/ml; *$P < .001$; 95% CI 86.9 to 153.9; P301S+LPS: +136.7 pg/ml; *$P < .001$; 95% CI 94.3 to 179.2) (n = 6/group). (F) *Il1b* mRNA levels were not elevated in the cortex or spinal cord of P301S compared to C57BL/6 mice. LPS injection increased *Il1b* in C57BL/6 mice (22.4-fold; $P < .001$; 95% CI 16.2 to 26.4) and P301S mice (9.5-fold; $P < .001$; 95% CI 6.4 to 12.5). LPS had a significantly smaller impact on *Il1b* in P301S than C57BL/6 mice (n = 6 for each group). Representative examples of AT8-stained cortical tissue (H–K) and spinal cord (M–P) collected 24 hours after injection from C57BL/6+saline, C57BL/6+LPS, P301S+saline, P301S+LPS mice. (L) AT8$^+$ cells were detected in the motor cortex (4.0 cells/mm^2; $P = .193$; 95% CI −2.6 to 10.7). LPS increased AT8$^+$ number in P301S mice only (9.2 Δ cells/mm^2; †$P = .055$; 95% CI −0.3 to 18.6) (C57BL/6+saline n = 3, C57BL/6+LPS n = 5, P301S+saline n = 6, P301S+LPS n = 4). (Q) AT8$^+$ cells were detected in lamina 9 of the spinal cord (22.7 cells/mm^2; **$P = .005$; 95% CI 8.9 to 36.4) and LPS increased the number of AT8$^+$ cells in P301S mice although this was not statistically significant (+15.2 Δ cells/mm^2 vs. P301S+saline; $P = .147$; 95% CI −6.6 to 36.9) (C57BL/6+saline n = 3, C57BL/6+LPS n = 5, P301S+saline n = 7, P301S+LPS n = 6). Scale bar 100 μm. Analyses were by mixed-effects LR; *$P < .05$, **$P < .005$, ***$P < .001$. Abbreviations: LR, linear regression; LPC, lipopolysaccharide.

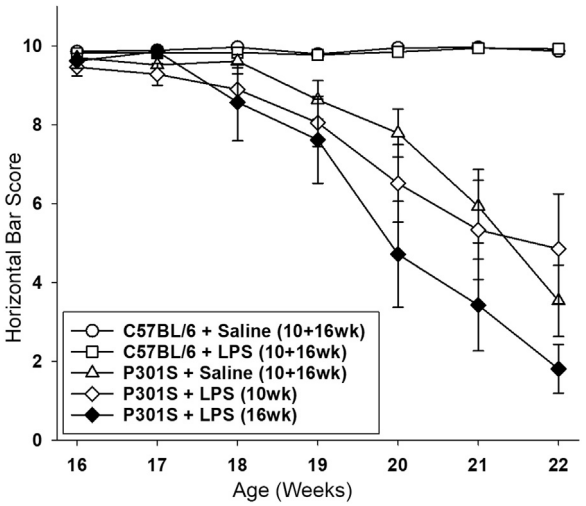

Fig. 4. LPS injection in P301S mice at 16 weeks, but not 10 weeks, accelerates decline of horizontal bar performance. P301S mice injected with saline (-△-) showed a steady performance decline (0.9 points/week; $P < .001$; 95% CI −1.0 to −0.8). LPS injection at 16 weeks, but not 10 weeks of age, accelerated decline in performance (P301S+LPS (10 wk) (-◇-): +0.1 Δ points/week versus P301S+saline; $P = .140$; 95% CI 0.0 to 0.2; P301S+LPS (16 wk) (-◆-): −0.5 Δ points/week versus P301S+saline; $P < .001$; 95% CI −0.6 to −0.4). The differential impact of age at LPS injection was significant when compared to C57BL/6 mice (−1.2 points/week; $P < .001$; 95% CI −1.3 to −1.0) and P301S mice (−0.6 points/week; $P < .001$; 95% CI −0.7 to −0.5) (≤20 weeks C57BL/6+saline n = 21, C57BL/6+LPS n = 22, P301S+saline n = 19, P301S+LPS (10 wk) n = 13, P301S+LPS (16 wk) n = 7; 21–22 weeks: C57BL/6+saline n = 18, C57BL/6+LPS n = 18, P301S+LPS (10 wk) n = 9, P301S+LPS (16 wk) n = 7). Analyses were by mixed-effects LR. Abbreviations: LR, linear regression; LPS, lipopolysaccharide.

Susceptibility to acute deficits and accelerated progression was independent of microglial priming or IL-1β hyperexpression after LPS injection.

4.1. Systemic inflammation and exacerbation of disease

Severe sepsis can induce acute brain failure, evident as delirium [27], permanent brain damage, and cognitive dysfunction in man and mouse [28]. Rodents injected with high-dose LPS to mimic severe sepsis developed CNS inflammation, BBB breakdown, neuronal death, and cognitive impairments [29–32]; however, precisely how these inflammatory insults impact the trajectory of neurological and functional decline is unknown. Here we show that a systemic low-dose LPS injection at 10 or 16 weeks of age caused an exaggerated, prolonged acute sickness response in P301S mice compared with controls. Importantly, these exaggerated acute symptoms extended beyond typical sickness behaviours to include motor symptoms; performance on the horizontal bar task was progressively impaired in P301S mice in late disease due to tauopathy-induced neurological dysfunction (Fig. 1), but this feature was absent at the time of LPS injection. Therefore, acute systemic inflammation unmasks disease-associated network vulnerability in presymptomatic animals, mirroring findings in the ME7 model of prion disease [12,18]. Findings, in both models support the idea that disease pathology progressively depletes cognitive and/or functional reserve rendering functions in those newly pathological regions vulnerable to acute stressors like LPS. There is also support for this in humans: baseline Mini–Mental State Examination score correlates strongly with delirium risk in older adults [18]. Although delirium is one major consequence of acute illness in dementia, patients also show marked impairment of trunk strength and motor function [33]. Given the vulnerability of motor function in the tauopathy model, acute failure in motor function during LPS-induced systemic inflammation illustrates a deleterious interaction of acute systemic inflammation with disease pathology, the magnitude of which is determined by the extent of the underlying pathology at the time of the acute inflammatory episode.

4.2. Microglia

We hypothesized that acute functional deficit might be underpinned by microglial priming. Previous studies demonstrated that microglial "priming" by primary neuropathology produces an exaggerated IL-1β response to subsequent inflammatory challenge [34], a phenotype replicated in multiple models [35–41], and shown by coexpression meta-analysis to share a transcriptional profile among several degenerative models, including the rTg4510 model [42]. Analysis of microglia in the present study demonstrated region-specific microgliosis: $IBA1^+$-microglial number in the cortex was unchanged at each time point analysed, even after LPS injection, while spinal cord $IBA1^+$-microglia showed progressive increase in number, morphological changes associated with activation, and increased expression of *Axl, Clec7a*, and *Itgax* genes, markers of primed microglia, and *Tyrobp*, a proxy for microglial number [42]. Conversely, cortical microglia maintained a ramified morphology throughout, and of the markers of priming, only *Itgax* expression was slightly elevated. Microglia exist on a spectrum of immune-vigilance along the rostral-caudal axis, such that cortical microglia are subject to stringent immune-regulation, whereas caudal microglia are more readily activated [43,44]. Our data also support work from pure tauopathy human postmortem studies where spatiotemporal correlation between microglial burden and pathological tau burden has been repeatedly observed [45–47]. However, although the immunohistochemical and transcriptional data demonstrate a primed microglial profile in the spinal cord but not in the cortex; upon systemic LPS challenge, neither region showed exaggerated *Il1b* transcription typical of primed microglia. Indeed, in both regions, *Il1b* transcription was significantly reduced in LPS-treated P301S mice with respect to LPS-treated controls, suggesting that microglia in the P301S model are desensitized by exposure to tau and/or degenerating neurons. Desensitization of microglia can occur upon repeated inflammatory challenge [48], and

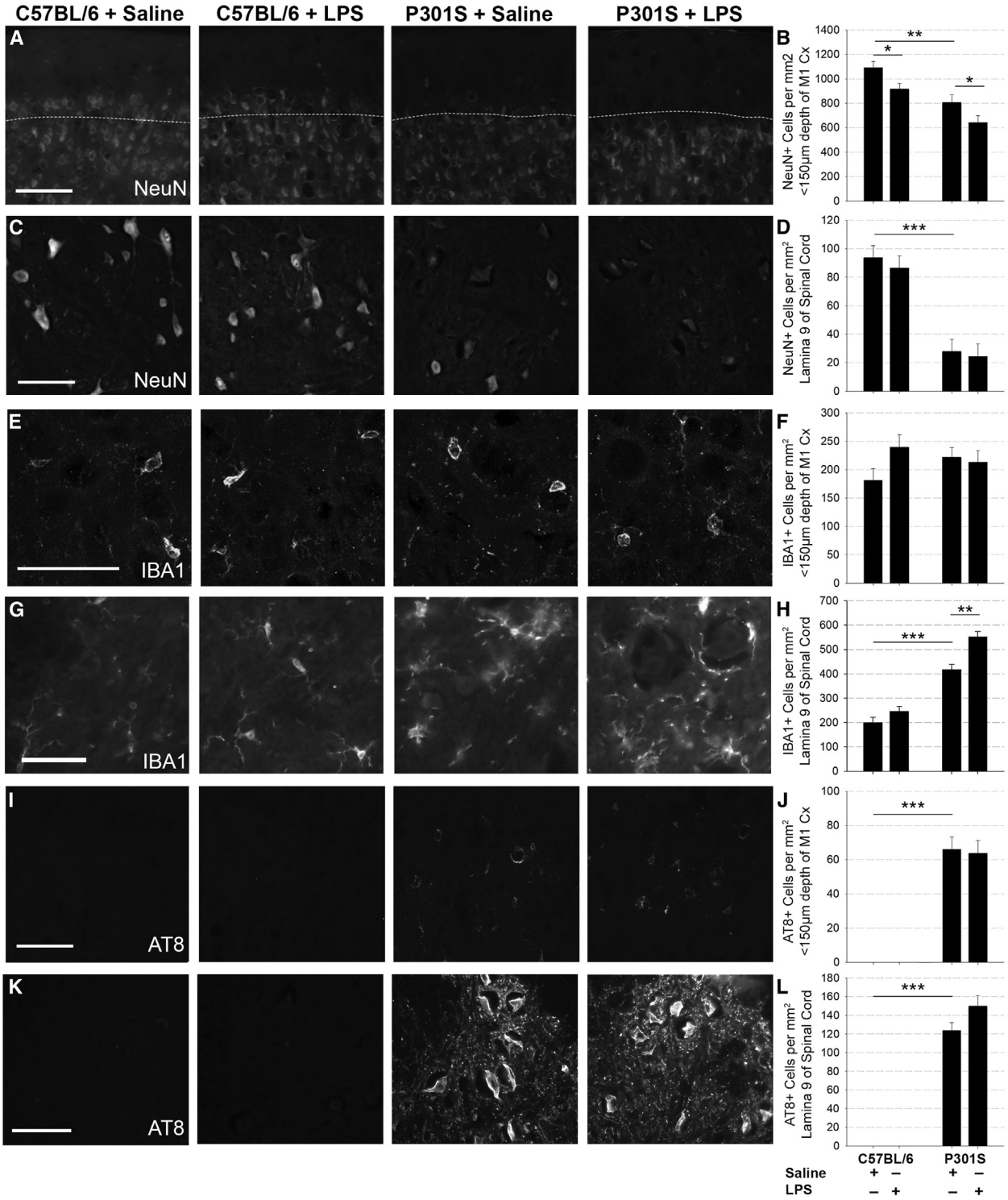

Fig. 5. Systemic inflammation exacerbates end-stage pathology: Representative examples of NeuN-stained (A and C), IBA1-stained (E and G), and AT8-stained (I and K) cortical and spinal cord tissue collected at 22 weeks of age from C57BL/6+saline, C57BL/6+LPS, P301S+saline, and P301S+LPS mice. Scale bars represent 100 µm (A, C, I, K) or 50 µm (E, G). (B) $NeuN^+$ cell counts in the motor cortex from C57BL/6 and P301S mice injected with either saline or LPS demonstrated significant neuronal loss in P301S mice compared with controls (-283.1 Δ cells/mm^2 vs. C57BL/6; $^{**}P < .005$; 95% CI -452.8 to -113.5). LPS impacted $NeuN^+$ cell counts in C57BL/6 mice, and P301S mice ($^{*}P < .05$), but there was no significant difference between genotypes (C57BL/6+saline n = 6, C57BL/6+LPS n = 7, P301S+saline n = 4, P301S+LPS n = 5). (D) $NeuN^+$ cell counts in lamina 9 of the spinal cord showed significant neuronal loss in P301S mice compared with controls (-65.9 Δ cells/mm^2; $^{***}P < .001$; 95% CI -90.8 to -41.0) but no effect of LPS on $NeuN^+$ cell counts (C57BL/6+saline n = 8, C57BL/6+LPS n = 8, P301S+saline n = 8, P301S+LPS n = 8). (F) $IBA1^+$ cell counts in the motor cortex 24 hours after injection indicate that neither genotype nor LPS exposure significantly impacted microgliosis (C57BL/6+saline n = 6, C57BL/6+LPS n = 7, P301S+saline n = 6, P301S+LPS n = 6). (H) $IBA1^+$ cell counts in the spinal cord lamina 9 demonstrate increased microgliosis in P301S compared to control mice (+218.7 Δ

there is some evidence that microglia in humans who died with terminal systemic infections also show an immunosuppressed phenotype [49]. Moreover, in AD tissue, hippocampal microglia proximal to tau pathology showed a dystrophic or degenerative profile which was partially replicated in Thy1-tau22, but not APP/PS1mice [50] indicating that tau does not affect microglia in the same way that amyloid-β does.

By end stage (22 weeks), there was profound microgliosis in the spinal cords of P301S mice, significantly increased after LPS treatment at 16 weeks, demonstrating that acute systemic inflammation drives tauopathy-related pathology. Although it is clear that tau can drive microgliosis [45–47,51–54], there is also evidence that microgliosis drives tau pathology [15,55]; hence, it is conceivable that an acute increase in tau pathology after LPS administration initiates a self-perpetuating loop between microgliosis and increasing tau pathology.

4.3. Exacerbation of tau pathology and functional decline by acute inflammation

A single LPS injection at 16 weeks acutely increased $AT8^+$-tau hyperphosphorylation in the motor cortex and spinal cords of P301S mice (Fig. 3H–Q). Transient tau hyperphosphorylation in response to systemic inflammation is described even in wild-type mice [56]. In 3xTg-AD mice, systemic LPS injection markedly increased tau hyperphosphorylation early in disease, mediated by dysregulation of tau kinase CDK5 [14], and later in disease attributed to GSK-3β activation [41]. In hTau transgenic mice, LPS-induced tau hyperphosphorylation 24-hours after injection was blocked in *Tlr4*$^{-/-}$ and *Il-1r1*$^{-/-}$ mice, implicating both canonical TLR4 and IL-1RI signalling [15]. In the present study, LPS induced robust *Il1b* mRNA expression in the cortices and spinal cords of C57BL/6 and P301S mice. Although *Il1b* expression was similar in P301S and C57BL/6 mice, one might still speculate that IL-1β could drive the observed exaggerated functional deficits: neurons from the degenerating brain were significantly more sensitive to IL-1β stimulation in other models [17]; hence, it is plausible that IL-1β levels innocuous in the healthy brain may damage neurons in disease. However, experiments in IL-1R1$^{-/-}$ mice show cytokine redundancy in LPS-induced neurological deficits; wild-type and IL-1R1$^{-/-}$ mice with ME7 prion disease injected with LPS developed equivalent sickness, weight loss, and acute working memory deficits [17] suggesting that alternative LPS-induced inflammatory mediators underpin exaggerated functional deficits in P301S mice.

4.4. Limitations and future work

This work has some limitations. Although we demonstrate that a single inflammatory episode causes significant alteration of disease course in a tauopathy model, we do not provide a complete mechanistic explanation. We propose contributions of proinflammatory cytokines, notably IL-1β that merits further exploration in this model of tauopathy. It is important to note that prior mechanistic studies of systemic inflammation–induced disease exacerbation in mutant tau models used higher LPS doses [15] or more numerous LPS challenges (500 μg/kg 2x/week for 6 weeks [14,41]). Therefore, our LPS dosing schedule, by design, likely better mimics the impact of a single episode of illness upon evolving tau-mediated pathology but it remains important to clarify mechanistic underpinning of these exacerbations. Moreover, it is now pressing to examine, in clinical populations with tau-mediated pathologies, whether acute inflammatory events such as infections, surgery, and inflammatory traumas produce acute changes in tau phosphorylation or other brain injury biomarkers that impact disease course.

4.5. Concluding remarks

The notion that a single systemic inflammatory event can produce acute functional deficits, can exacerbate disease-associated pathology, and can hasten terminal functional decline, shown here in P301S mice and supported in AD patients [10], illustrates the potential of acute illness to accelerate disease progression and emphasizes that there are likely important therapeutic targets for slowing down progression of dementia that are tractable from outside the CNS. Inflammation is a component of numerous preventable medical conditions including hypertension, hypercholesterolemia, diabetes, and obesity [8]; prevention or treatment of which might reduce dementia incidence and improve cognitive health with huge potential impact [57].

Acknowledgments

The authors would like to thank Professor B. Paul Morgan for constructive criticism of the manuscript. The authors would like to acknowledge Professor Maria Spillantini and Dr Michel Goedert for providing the P301S tau mouse line. Megan Torvell was supported by a PhD studentship from the University of Edinburgh Centre for Cognitive Aging and Cognitive Epidemiology, part of the cross council Lifelong

cells/mm^2; ***$P < .001$; 95% CI 153.7 to 283.7), further increased in response to LPS, more in P301S than controls (+133.6 Δ cells/mm^2; **$P = .003$; 95% CI 52.7 to 214.6 vs. + 87.5 Δ cells/mm^2; $P = .061$; 95% CI −4.4 to 179.3). C57BL/6+saline n = 8, C57BL/6+LPS n = 8, P301S+saline n = 8, P301S+LPS n = 7. $AT8^+$ cells were detected in the motor cortex (J) and spinal cord (L) of P301S mice (cortex: 65.8 cells/mm^2; ***$P < .001$; 95% CI 48.6 to 83.1; spinal cord: 123.8 cells/mm^2; $P < .001$; 95% CI 101.2 to 146.4). LPS did not impact this aspect of tau pathology (I and K). Analyses were by mixed-effects LR; *$P < .05$, **$P < .005$, ***$P < .001$. Abbreviations: LR, linear regression; LPS, lipopolysaccharide.

Health and Wellbeing Initiative (MR/L501530/1). Funding from the Biotechnology and Biological Sciences Research Council (BBSRC) and Medical Research Council (MRC) is gratefully acknowledged. Funding was also provided by the Euan Macdonald Centre at the University of Edinburgh.

Supplementary data

Supplementary data related to this article can be found at https://doi.org/10.1016/j.trci.2019.09.001.

RESEARCH IN CONTEXT

1. Systematic review: The authors reviewed the literature using traditional methods to identify evidence implicating systemic inflammation as a trigger of acute and chronic behavioural and pathological effects in the context of neurodegeneration. This phenomenon is described in dementia models and may depend on microglial priming. Our study is the first to examine functional decline in a pure tauopathy neurodegeneration model.
2. Interpretation: Our findings support a significant negative impact of a single systemic inflammatory episode on subsequent disease course in the tauopathy model; inflammation was independent of microglial priming. We conclude that systemic inflammation exacerbates chronic decline in the model.
3. Future directions: The manuscript describes exaggerated neurological deficits induced by a single inflammatory episode; future work would prioritize understanding the specific contributions of brain endothelium, astrocytes, microglia, and infiltrating immune cells and whether the observed deficits result from intrinsic tau-mediated neuronal injury or exaggerated extrinsic neuroinflammatory factors.

References

[1] Lambert J-C, Ibrahim-Verbaas CA, Harold D, Naj AC, Sims R, Bellenguez C, et al. Meta-analysis of 74,046 individuals identifies 11 new susceptibility loci for Alzheimer's disease. Nat Genet 2013; 45:1452–8.
[2] Lambert J-C, Heath S, Even G, Campion D, Sleegers K, Hiltunen M, et al. Genome-wide association study identifies variants at CLU and CR1 associated with Alzheimer's disease. Nat Genet 2009;41:1094–9.
[3] Karch CM, Goate AM. Alzheimer's disease risk genes and mechanisms of disease pathogenesis. Biol Psychiatry 2015;77:43–51.
[4] Jun G, Naj AC, Beecham GW, Wang LS, Buros J, Gallins PJ, et al. Meta-analysis confirms CR1, CLU, and PICALM as Alzheimer disease risk loci and reveals interactions with APOE genotypes. Arch Neurol 2010;67:1473–84.
[5] Guerreiro R, Wojtas A, Bras J, Carrasquillo M, Rogaeva E, Majounie E, et al. TREM2 Variants in Alzheimer's disease. N Engl J Med 2012;368:117–27.
[6] Jonsson T, Stefansson H, Steinberg S, Jonsdottir I, Jonsson PV, Snaedal J, et al. Variant of TREM2 associated with the risk of Alzheimer's disease. N Engl J Med 2013;368:107–16.
[7] Singaraja RR. TREM2: a new risk factor for Alzheimer's disease. Clin Genet 2013;83:525–6.
[8] Dunn N, Mullee M, Perry VH, Holmes C. Association between dementia and infectious disease: evidence from a Case-Control Study. Alzheimer Dis Assoc Disord 2005;19:91–4.
[9] Engelhart MJ, Geerlings MI, Meijer J, Kiliaan A, Ruitenberg A, van Swieten JC, et al. Inflammatory proteins in plasma and the risk of dementia: the rotterdam study. Arch Neurol 2004;61:668–72.
[10] Walker KA, Gottesman RF, Wu A, Knopman DS, Gross AL, Mosley TH, et al. Systemic inflammation during midlife and cognitive change over 20 years. The ARIC Study. Neurology 2019; 92:e1256–67.
[11] Holmes C, Colm C, Zotova E, Woolford J, Dean C, Kerr S, et al. Systemic inflammation and disease progression in Alzheimer disease. Neurology 2009;73:768–74.
[12] Cunningham C, Campion S, Lunnon K, Murray CL, Woods JFC, Deacon RMJ, et al. Systemic inflammation induces acute behavioral and cognitive changes and accelerates neurodegenerative disease. Biol Psychiatry 2009;65:304–12.
[13] Perry VH, Cunningham C, Holmes C. Systemic infections and inflammation affect chronic neurodegeneration. Nat Rev Immunol 2007;7:161–7.
[14] Kitazawa M, Oddo S, Yamasaki TR, Green KN, LaFerla FM. Lipopolysaccharide-induced inflammation exacerbates tau pathology by a cyclin-dependent kinase 5-mediated pathway in a transgenic model of Alzheimer's disease. J Neurosci 2005;25:8843–53.
[15] Bhaskar K, Konerth M, Kokiko-Cochran ON, Cardona A, Ransohoff RM, Lamb BT. Regulation of tau pathology by the microglial fractalkine receptor. Neuron 2010;68:19–31.
[16] Lee DC, Rizer J, Selenica M-LB, Reid P, Kraft C, Johnson A, et al. LPS- induced inflammation exacerbates phospho-tau pathology in rTg4510 mice. J Neuroinflammation 2010;7:56.
[17] Skelly DT, Griffin EW, Murray CL, Harney S, O'Boyle C, Hennessy E, et al. Acute transient cognitive dysfunction and acute brain injury induced by systemic inflammation occur by dissociable IL-1-dependent mechanisms. Mol Psychiatry 2018;24:1533–48.
[18] Davis DH, Skelly DT, Murray C, Hennessy E, Bowen J, Norton S, et al. Worsening cognitive impairment and neurodegenerative pathology progressively increase risk for delirium. Am J Geriatr Psychiatry 2015;23:403–15.
[19] Hampton DW, Webber DJ, Bilican B, Goedert M, Spillantini MG, Chandran S. Cell-mediated neuroprotection in a mouse model of human tauopathy. J Neurosci 2010;30:9973–83.
[20] Allen B, Ingram E, Takao M, Smith MJ, Jakes R, Virdee K, et al. Abundant tau filaments and nonapoptotic neurodegeneration in transgenic mice expressing human P301S tau protein. J Neurosci 2002; 22:9340–51.
[21] Bellucci A, Westwood AJ, Ingram E, Casamenti F, Goedert M, Spillantini Maria G. Induction of inflammatory mediators and microglial activation in mice transgenic for mutant human P301S tau protein. Am J Pathol 2004;165:1643–52.
[22] Murray CL, Skelly DT, Cunningham C. Exacerbation of CNS inflammation and neurodegeneration by systemic LPS treatment is independent of circulating IL-1β and IL-6. J Neuroinflammation 2011;8:50.
[23] Paxinos G, Franklin KB. The Mouse Brain in Stereotaxic Coordinates. Cambridge, MA: Gulf professional publishing; 2004.
[24] Schindelin J, Arganda-Carreras I, Frise E, Kaynig V, Longair M, Pietzsch T, et al. Fiji: an open-source platform for biological-image analysis. Nat Methods 2012;9:676–82.

[25] Schneider CAR WS, Eliceiri KW. NIH Image to ImageJ: 25 years of image analysis. Nat Methods 2012;9:671–5.
[26] Schmittgen TD, Livak KJ. Analyzing real-time PCR data by the comparative CT method. Nat Protoc 2008;3:1101–8.
[27] Iwashyna TJ, Ely EW, Smith DM, Langa KM. Long-term cognitive impairment and functional disability among survivors of severe sepsis. JAMA 2010;304:1787–94.
[28] Widmann CN, Heneka MT. Long-term cerebral consequences of sepsis. Lancet Neurol 2014;13:630–6.
[29] d'Avila JC, Siqueira LD, Mazeraud A, Azevedo EP, Foguel D, Castro-Faria-Neto HC, et al. Age-related cognitive impairment is associated with long-term neuroinflammation and oxidative stress in a mouse model of episodic systemic inflammation. J Neuroinflammation 2018;15:28.
[30] Polito A, Lorin de la Grandmaison G, Mansart A, Louiset E, Lefebvre H, Sharshar T, et al. Human and experimental septic shock are characterized by depletion of lipid droplets in the adrenals. Intensive Care Med 2010;36:1852–8.
[31] Semmler A, Frisch C, Debeir T, Ramanathan M, Okulla T, Klockgether T, et al. Long-term cognitive impairment, neuronal loss and reduced cortical cholinergic innervation after recovery from sepsis in a rodent model. Exp Neurol 2007;204:733–40.
[32] Semmler A, Okulla T, Sastre M, Dumitrescu-Ozimek L, Heneka MT. Systemic inflammation induces apoptosis with variable vulnerability of different brain regions. J Chem Neuroanat 2005; 30:144–57.
[33] Bellelli G, Speciale S, Morghen S, Torpilliesi T, Turco R, Trabucchi M. Are fluctuations in motor performance a diagnostic sign of delirium? J Am Med Dir Assoc 2011;12:578–83.
[34] Cunningham C, Wilcockson DC, Campion S, Lunnon K, Perry VH. Central and systemic endotoxin challenges exacerbate the local inflammatory response and increase neuronal death during chronic neurodegeneration. J Neurosci 2005;25:9275–84.
[35] Godbout JP, Chen J, Abraham J, Richwine AF, Berg BM, Kelley KW, et al. Exaggerated neuroinflammation and sickness behavior in aged mice following activation of the peripheral innate immune system. FASEB J 2005;19:1329–31.
[36] Pott Godoy MC, Tarelli R, Ferrari CC, Sarchi MI, Pitossi FJ. Central and systemic IL-1 exacerbates neurodegeneration and motor symptoms in a model of Parkinson's disease. Brain 2008; 131:1880–94.
[37] Palin K, Cunningham C, Forse P, Perry VH, Platt N. Systemic inflammation switches the inflammatory cytokine profile in CNS Wallerian degeneration. Neurobiol Dis 2008;30:19–29.
[38] Raj DDA, Jaarsma D, Holtman IR, Olah M, Ferreira FM, Schaafsma W, et al. Priming of microglia in a DNA-repair deficient model of accelerated aging. Neurobiol Aging 2014; 35:2147–60.
[39] Chen J, Buchanan JB, Sparkman NL, Godbout JP, Freund GG, Johnson RW. Neuroinflammation and disruption in working memory in aged mice after acute stimulation of the peripheral innate immune system. Brain Behav Immun 2008;22:301–11.
[40] Henry CJ, Huang Y, Wynne AM, Godbout JP. Peripheral lipopolysaccharide (LPS) challenge promotes microglial hyperactivity in aged mice that is associated with exaggerated induction of both pro-inflammatory IL-1beta and anti-inflammatory IL-10 cytokines. Brain Behav Immun 2009;23:309–17.
[41] Sy M, Kitazawa M, Medeiros R, Whitman L, Cheng D, Lane TE, et al. Inflammation induced by infection potentiates tau pathological features in transgenic mice. Am J Pathol 2011;178:2811–22.
[42] Holtman IR, Raj DD, Miller JA, Schaafsma W, Yin Z, Brouwer N, et al. Induction of a common microglia gene expression signature by aging and neurodegenerative conditions: a co-expression meta-analysis. Acta Neuropathol Commun 2015;3:31.
[43] Grabert K, Michoel T, Karavolos MH, Clohisey S, Baillie JK, Stevens MP, et al. Microglial brain region-dependent diversity and selective regional sensitivities to aging. Nat Neurosci 2016;19:504–16.
[44] Kim WG, Mohney RP, Wilson B, Jeohn GH, Liu B, Hong JS. Regional difference in susceptibility to lipopolysaccharide-induced neurotoxicity in the rat brain: role of microglia. J Neurosci 2000; 20:6309–16.
[45] Sasaki A, Kawarabayashi T, Murakami T, Matsubara E, Ikeda M, Hagiwara H, et al. Microglial activation in brain lesions with tau deposits: comparison of human tauopathies and tau transgenic mice TgTauP301L. Brain Res 2008;1214:159–68.
[46] Paulus W, Bancher C, Jellinger K. Microglial reaction in Pick's disease. Neurosci Lett 1993;161:89–92.
[47] Ishizawa K, Dickson DW. Microglial activation parallels system degeneration in progressive supranuclear palsy and corticobasal degeneration. J Neuropathol Exp Neurol 2001;60:647.
[48] Wendeln AC, Degenhardt K, Kaurani L, Gertig M, Ulas T, Jain G, et al. Innate immune memory in the brain shapes neurological disease hallmarks. Nature 2018;556:332–8.
[49] Rakic S, Hung YMA, Smith M, So D, Tayler HM, Varney W, et al. Systemic infection modifies the neuroinflammatory response in late stage Alzheimer's disease. Acta Neuropathol Commun 2018;6:88.
[50] Sanchez-Mejias E, Navarro V, Jimenez S, Sanchez-Mico M, Sanchez-Varo R, Nunez-Diaz C, et al. Soluble phospho-tau from Alzheimer's disease hippocampus drives microglial degeneration. Acta Neuropathol 2016;132:897–916.
[51] Morales I, Jimenez JM, Mancilla M, Maccioni RB. Tau oligomers and fibrils induce activation of microglial cells. J Alzheimers Dis 2013; 37:849–56.
[52] Ikeda M, Kawarai T, Kawarabayashi T, Matsubara E, Murakami T, Sasaki A, et al. Accumulation of filamentous tau in the cerebral cortex of human tau R406W transgenic mice. Am J Pathol 2005;166:521–31.
[53] Kida E, Barcikowska M, Niemczewska M. Immunohistochemical study of a case with progressive supranuclear palsy without ophthalmoplegia. Acta Neuropathol 1992;83:328–32.
[54] Sheng JG, Mrak RE, Griffin WST. Glial-neuronal interactions in Alzheimer disease: progressive association of IL-1α microglia and S100β astrocytes with neurofibrillary tangle stages. J Neuropathol Exp Neurol 1997;56:285.
[55] Maphis N, Xu G, Kokiko-Cochran ON, Jiang S, Cardona A, Ransohoff RM, et al. Reactive microglia drive tau pathology and contribute to the spreading of pathological tau in the brain. Brain 2015;138:1738–55.
[56] Roe AD, Staup MA, Serrats J, Sawchenko PE, Rissman RA. Lipopolysaccharide-induced tau phosphorylation and kinase activity–modulation, but not mediation, by corticotropin-releasing factor receptors. Eur J Neurosci 2011;34:448–56.
[57] Wu Y-T, Fratiglioni L, Matthews FE, Lobo A, Breteler MMB, Skoog I, et al. Dementia in western Europe: epidemiological evidence and implications for policy making. Lancet Neurol 2016;15:116–24.